

Introduction of luminescent rhenium(I), ruthenium(II), iridium(III) and rhodium(III) systems into rhodamine-tethere ligands for the construction of bichromophoric chemosensors

Chunyan Wang,<sup>a,b</sup> Ho-Chuen Lam,<sup>b</sup> Nianyong Zhu<sup>b</sup>, and Keith Man-Chung Wong<sup>a,b\*</sup>

<sup>a</sup> *Department of Chemistry, South University of Science and Technology of China, No. 1088, Tangchang Boulevard, Nanshan District, Shenzhen 518055, Guangdong, P.R. China*

<sup>b</sup> *Department of Chemistry, The University of Hong Kong, Pokfulam Road, Hong Kong, P.R. China*

## **Electronic supplementary information (ESI)**

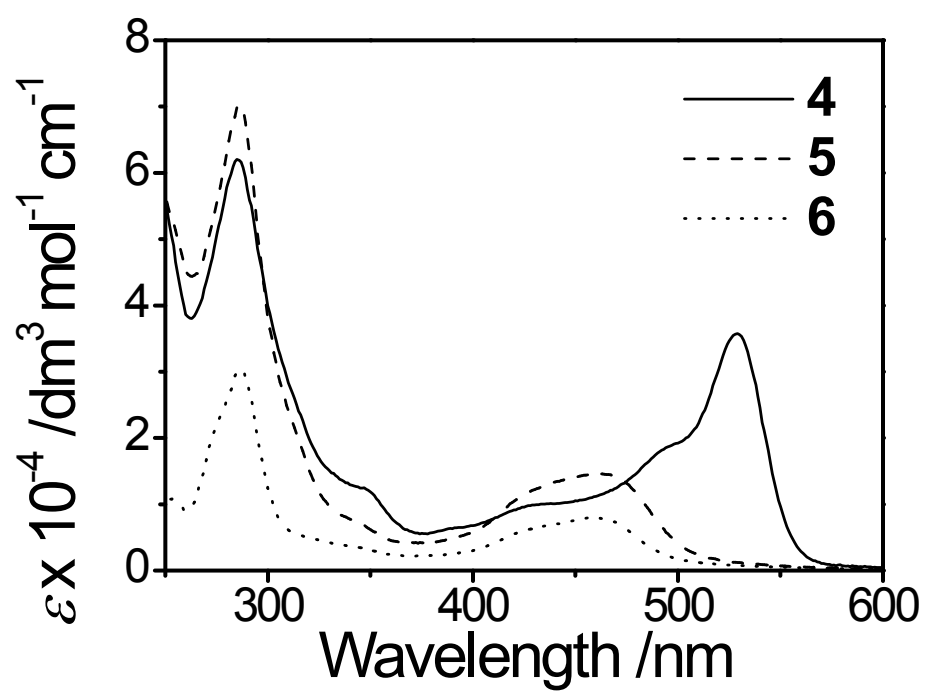


**Figure S1** Electronic absorption spectra of 4–6 in acetonitrile at 298 K

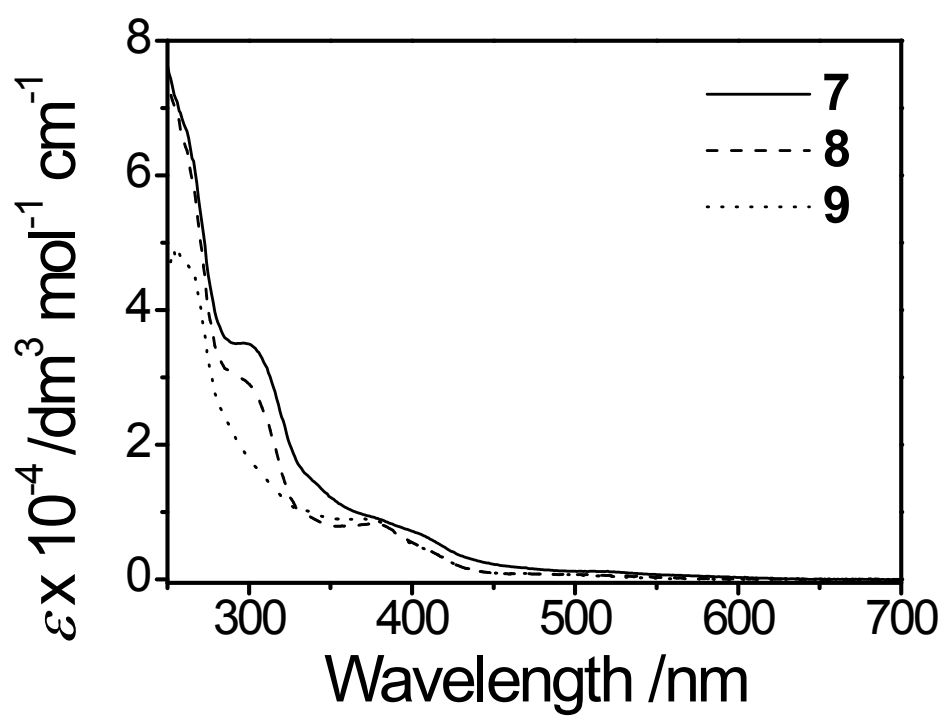


**Figure S2** Electronic absorption spectra of **7–9** in acetonitrile at 298 K

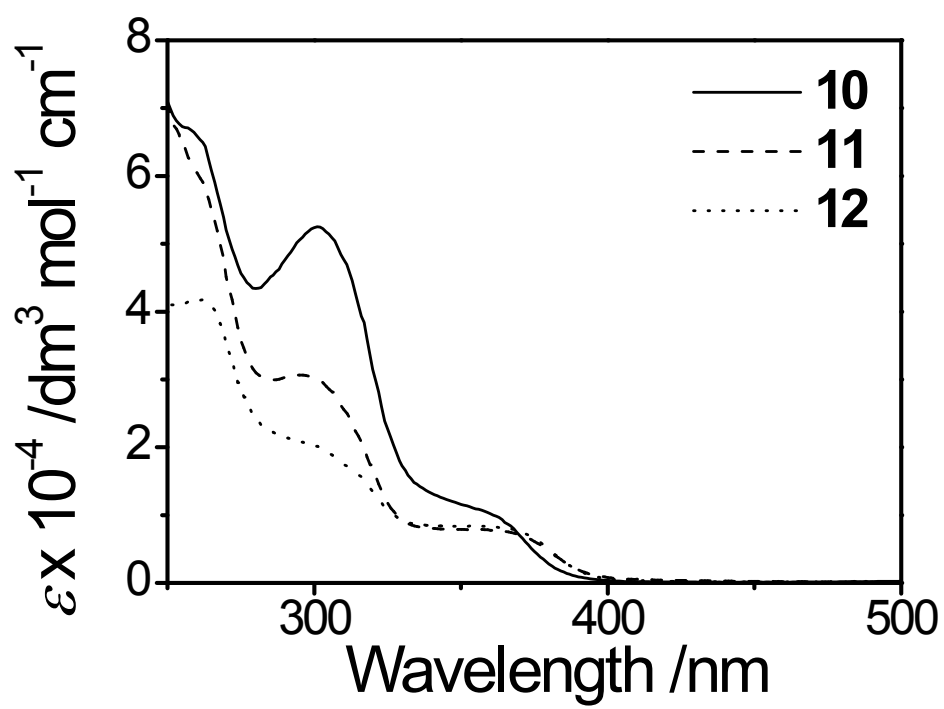


**Figure S3** Electronic absorption spectra of **10–12** in acetonitrile at 298 K

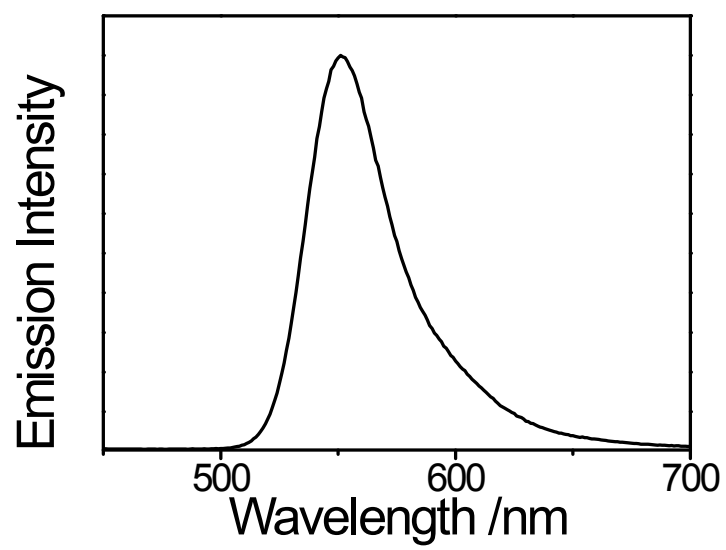


**Figure S4** The normalized emission spectrum of **4** in acetonitrile at 298 K

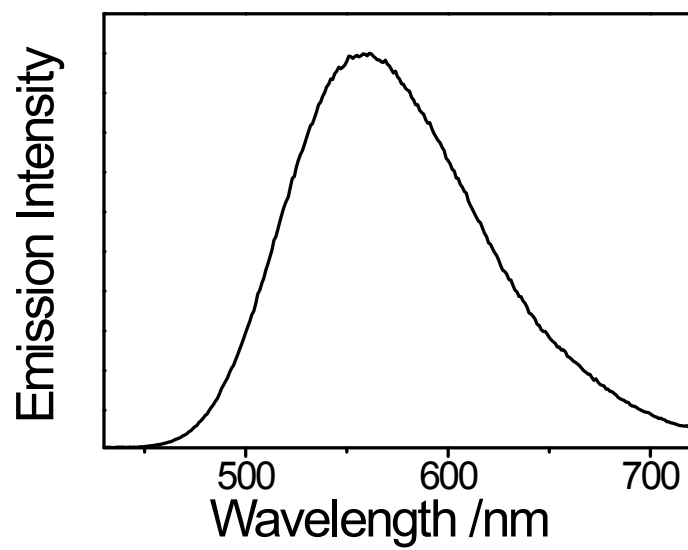


**Figure S5** The normalized emission spectrum of **12** in acetonitrile at 298 K

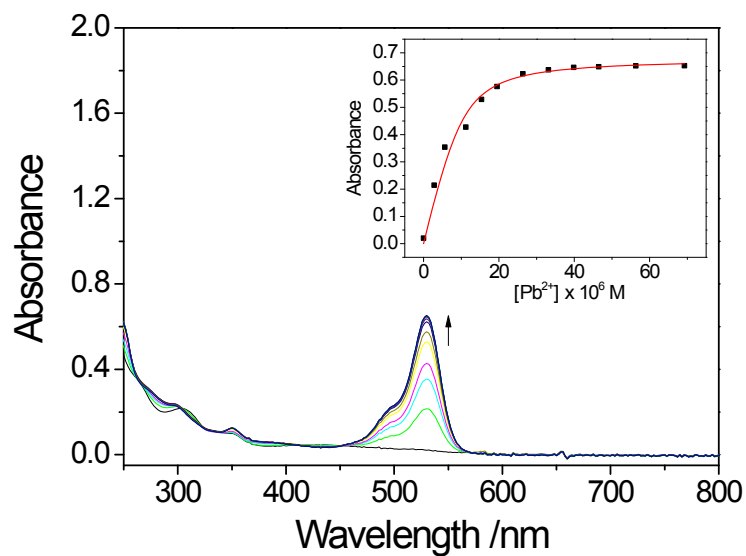


**Figure S6** Electronic absorption of **1** in  $\text{CH}_3\text{CN}$  (concentration =  $11.8 \mu\text{M}$ ) at 298 K upon addition of various concentrations of  $\text{Pb}^{2+}$ . Inset shows the plots of the absorbance at 530 nm as a function of the concentration of  $\text{Pb}^{2+}$ .

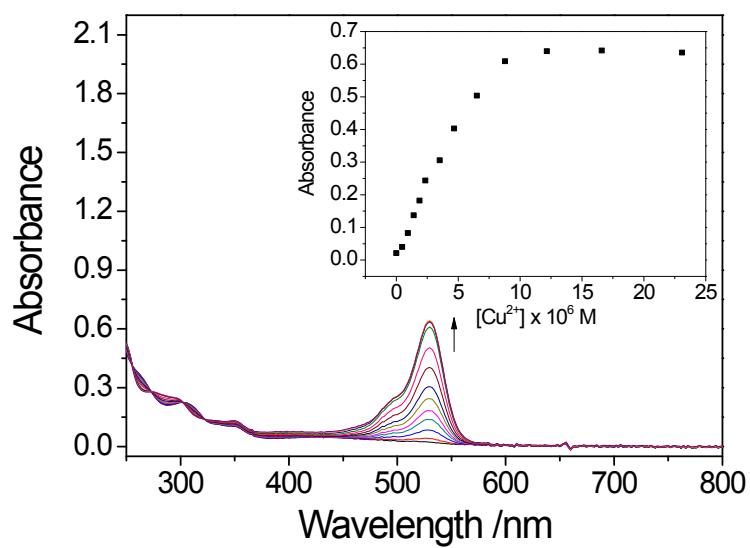


**Figure S7** Electronic absorption of **1** in  $\text{CH}_3\text{CN}$  (concentration =  $11.8 \mu\text{M}$ ) at 298 K upon addition of various concentrations of  $\text{Cu}^{2+}$ . Inset shows the plots of the absorbance at 530 nm as a function of the concentration of  $\text{Cu}^{2+}$ .



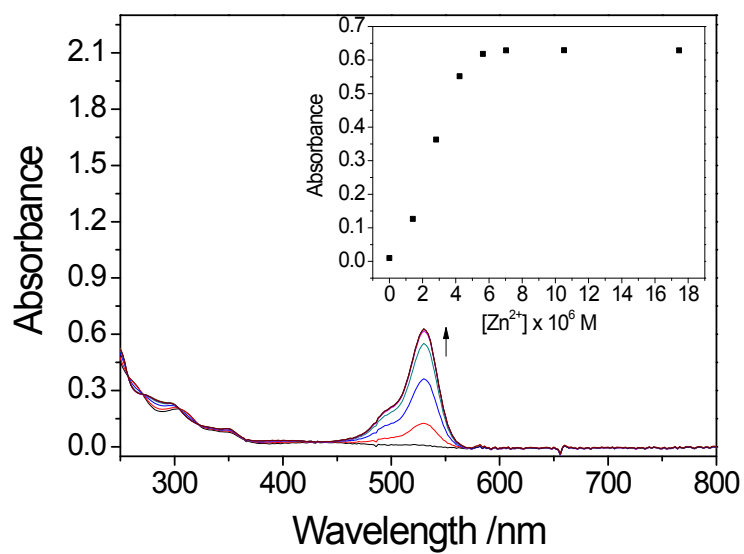


**Figure S8** Electronic absorption of **1** in  $\text{CH}_3\text{CN}$  (concentration =  $11.8 \mu\text{M}$ ) at 298 K upon addition of various concentrations of  $\text{Zn}^{2+}$ . Inset shows the plots of the absorbance at 530 nm as a function of the concentration of  $\text{Zn}^{2+}$ .

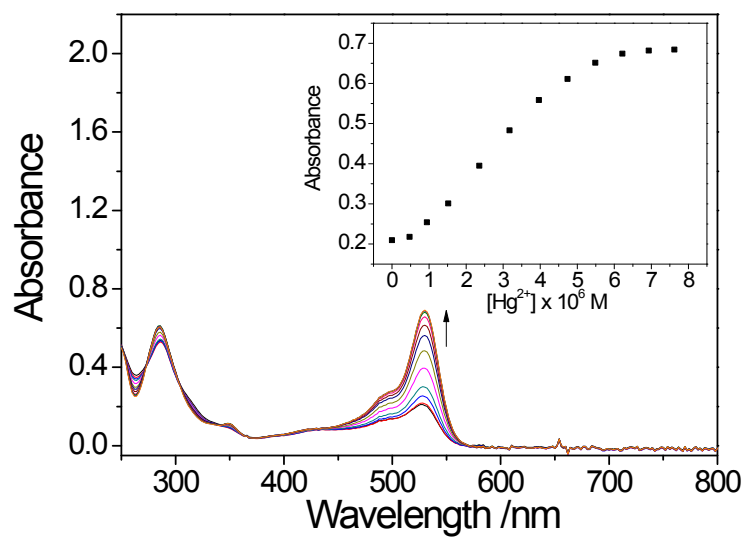


**Figure S8** Electronic absorption of **4** in  $\text{CH}_3\text{CN}$  (concentration =  $11.8 \mu\text{M}$ ) at 298 K upon addition of various concentrations of  $\text{Hg}^{2+}$ . Inset shows the plots of the absorbance at 530 nm as a function of the concentration of  $\text{Hg}^{2+}$ .

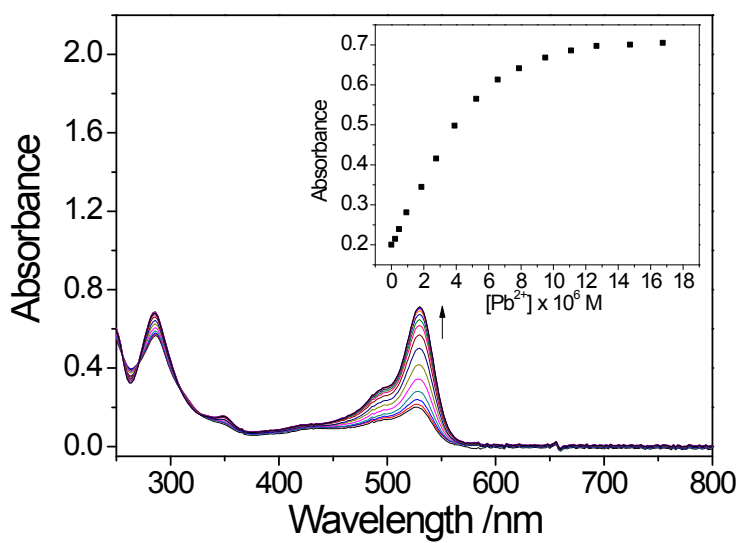


**Figure S9** Electronic absorption of **4** in  $\text{CH}_3\text{CN}$  (concentration =  $11.8 \mu\text{M}$ ) at 298 K upon addition of various concentrations of  $\text{Pb}^{2+}$ . Inset shows the plots of the absorbance at 530 nm as a function of the concentration of  $\text{Pb}^{2+}$ .

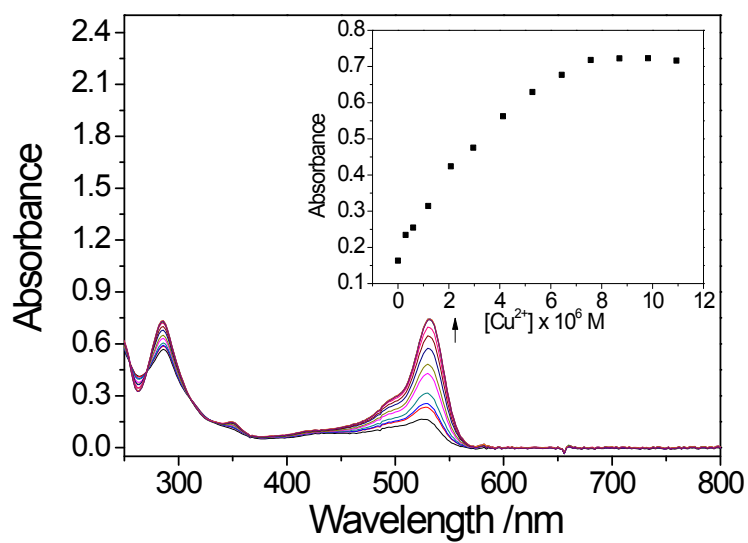


**Figure S10** Electronic absorption of **4** in  $\text{CH}_3\text{CN}$  (concentration =  $11.8 \mu\text{M}$ ) at 298 K upon addition of various concentrations of  $\text{Cu}^{2+}$ . Inset shows the plots of the absorbance at 530 nm as a function of the concentration of  $\text{Cu}^{2+}$ .

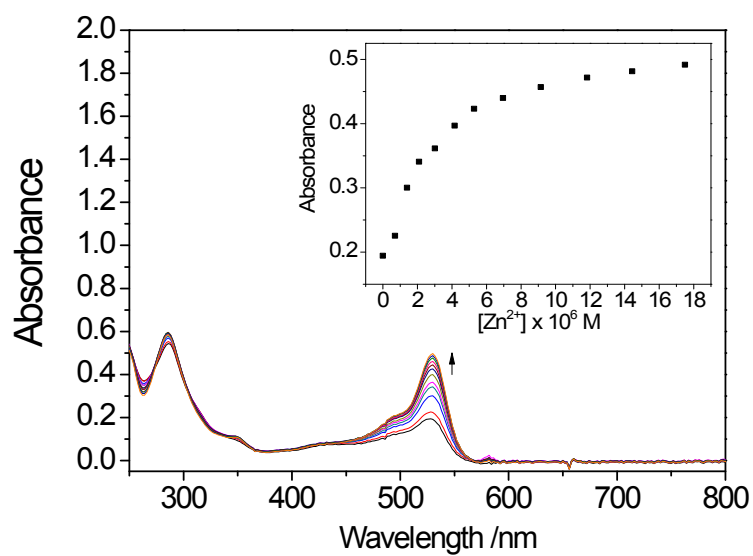


**Figure S11** Electronic absorption of **4** in CH<sub>3</sub>CN (concentration = 11.8  $\mu$ M) at 298 K upon addition of various concentrations of Zn<sup>2+</sup>. Inset shows the plots of the absorbance at 530 nm as a function of the concentration of Zn<sup>2+</sup>.

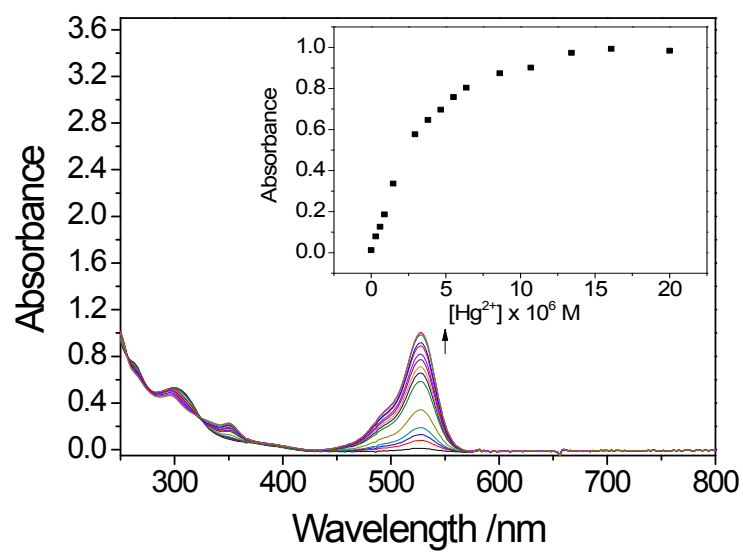


**Figure S12** Electronic absorption of **7** in CH<sub>3</sub>CN (concentration = 11.7  $\mu$ M) at 298 K upon addition of various concentrations of Hg<sup>2+</sup>. Inset shows the plots of the absorbance at 530 nm as a function of the concentration of Hg<sup>2+</sup>.

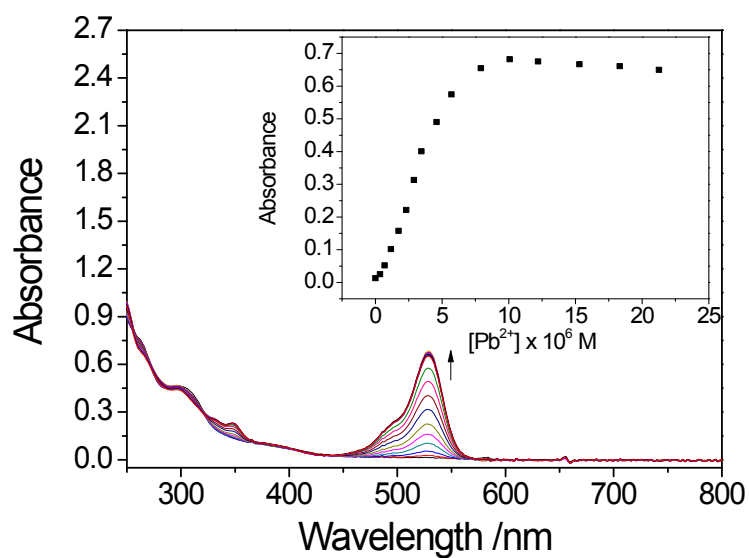


**Figure S13** Electronic absorption of **7** in  $\text{CH}_3\text{CN}$  (concentration =  $11.7 \mu\text{M}$ ) at 298 K upon addition of various concentrations of  $\text{Pb}^{2+}$ . Inset shows the plots of the absorbance at 530 nm as a function of the concentration of  $\text{Pb}^{2+}$ .

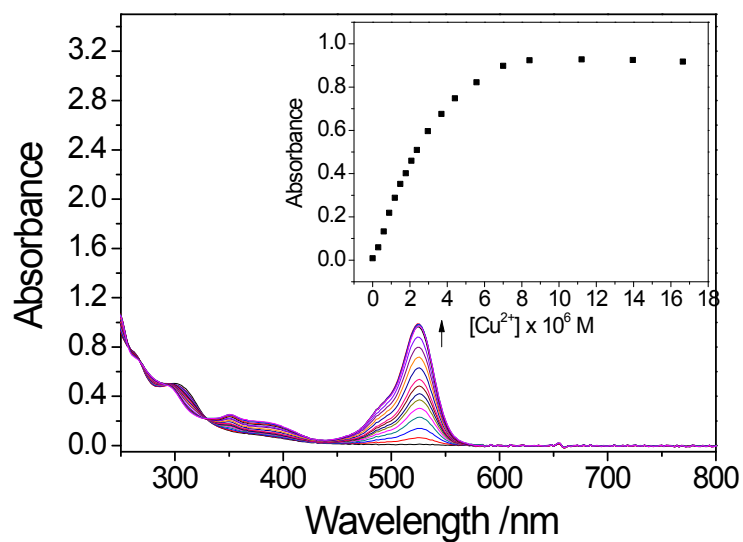


**Figure S14** Electronic absorption of **7** in CH<sub>3</sub>CN (concentration = 11.7  $\mu$ M) at 298 K upon addition of various concentrations of Cu<sup>2+</sup>. Inset shows the plots of the absorbance at 530 nm as a function of the concentration of Cu<sup>2+</sup>.



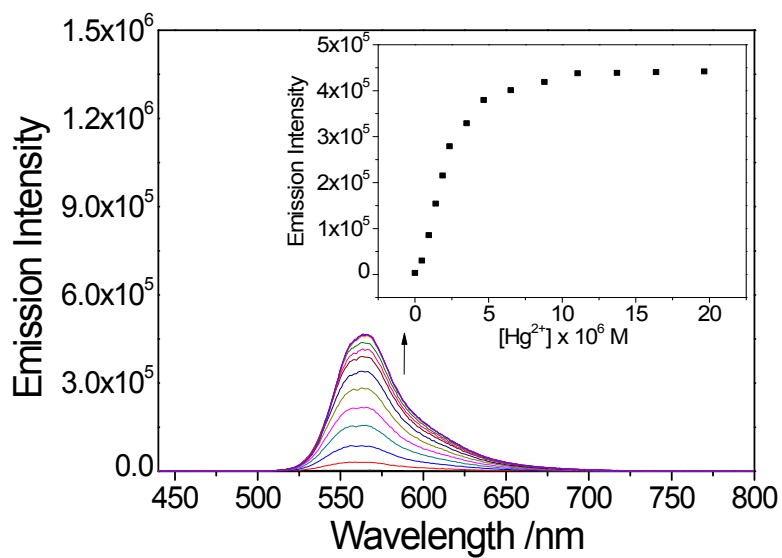


**Figure S15** Corrected emission spectra of **1** ( $9.66 \mu\text{M}$ ) in acetonitrile at 298 K upon addition of various concentrations of  $\text{Hg}^{2+}$ . Inset shows the plots of the emission intensity at 560 nm as a function of the concentration of  $\text{Hg}^{2+}$ .

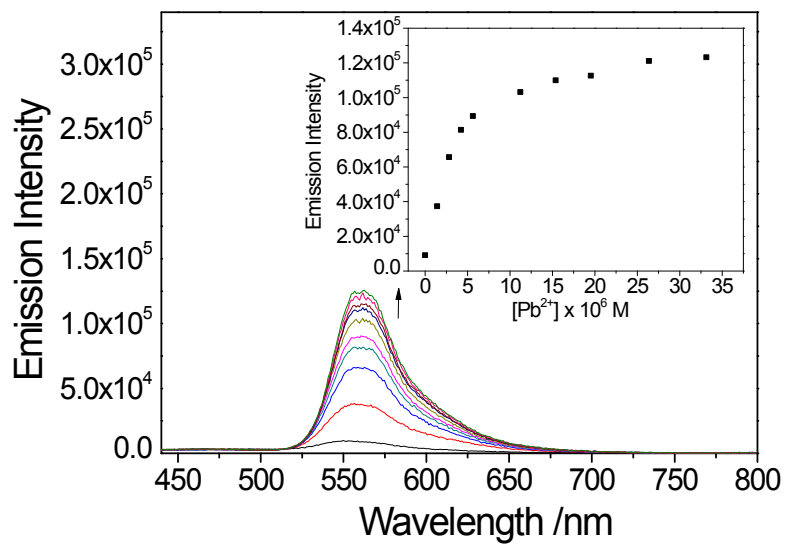


**Figure S16** Corrected emission spectra of **1** (11.8 μM) in acetonitrile at 298 K upon addition of various concentrations of Pb<sup>2+</sup>. Inset shows the plots of the emission intensity at 560 nm as a function of the concentration of Pb<sup>2+</sup>.

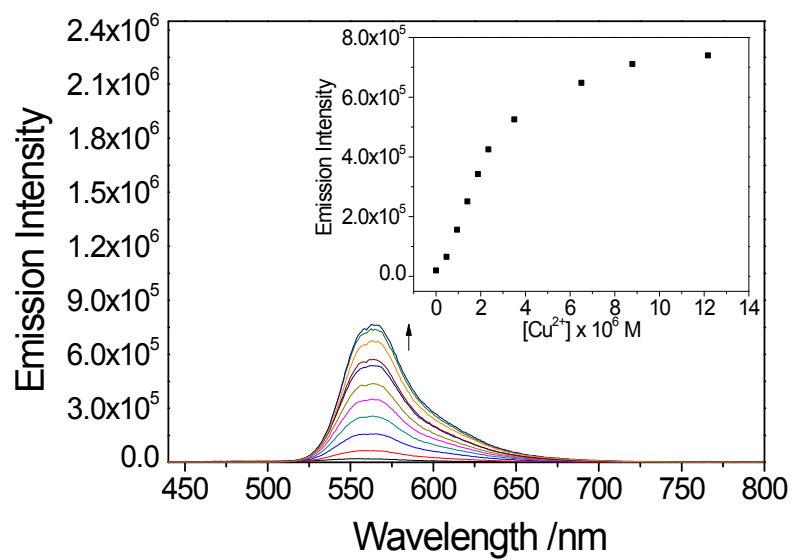


**Figure S17** Corrected emission spectra of **1** (11.8  $\mu\text{M}$ ) in acetonitrile at 298 K upon addition of various concentrations of  $\text{Cu}^{2+}$ . Inset shows the plots of the emission intensity at 560 nm as a function of the concentration of  $\text{Cu}^{2+}$ .

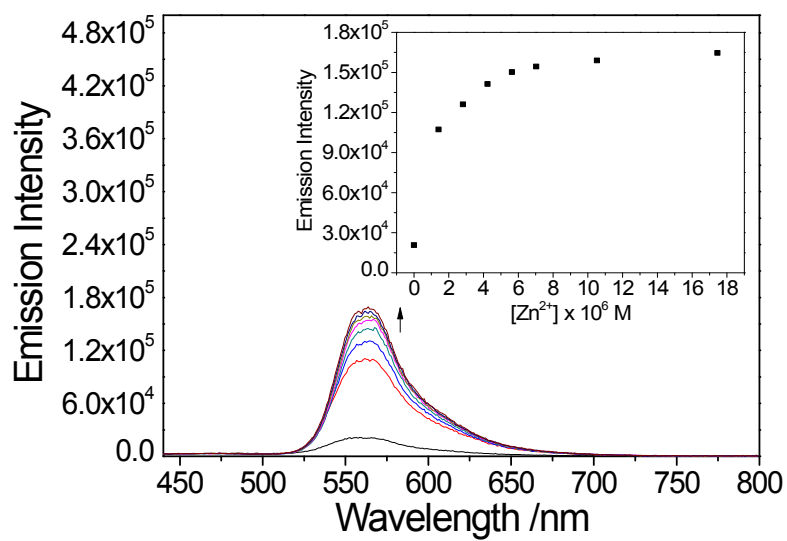


**Figure S18** Corrected emission spectra of **1** (11.8  $\mu\text{M}$ ) in acetonitrile at 298 K upon addition of various concentrations of  $\text{Zn}^{2+}$ . Inset shows the plots of the emission intensity at 560 nm as a function of the concentration of  $\text{Zn}^{2+}$ .

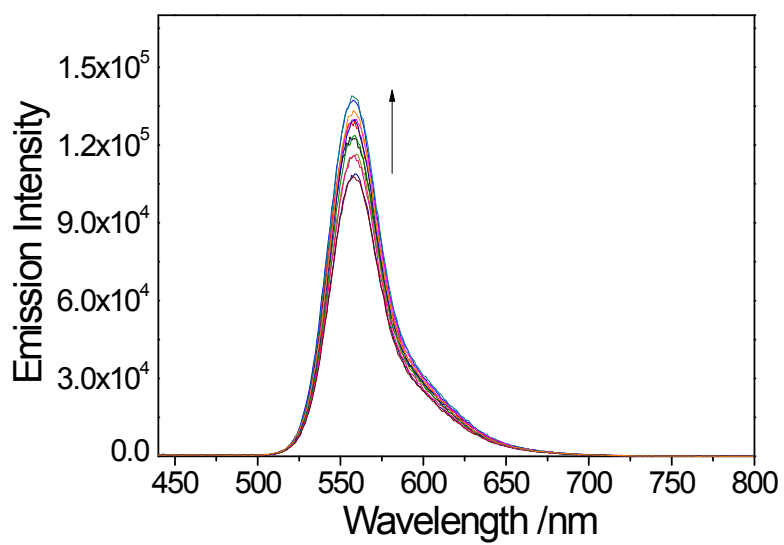


**Figure S19** Corrected emission spectra of **4** (11.8 μM) in acetonitrile at 298 K upon addition of various concentrations of Hg<sup>2+</sup>.

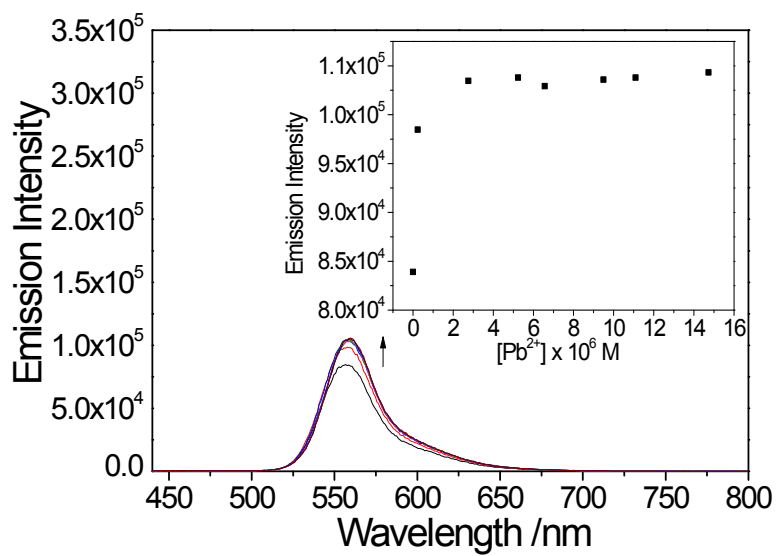


**Figure S20** Corrected emission spectra of **4** (11.8 μM) in acetonitrile at 298 K upon addition of various concentrations of Pb<sup>2+</sup>. Inset shows the plots of the emission intensity at 560 nm as a function of the concentration of Pb<sup>2+</sup>.

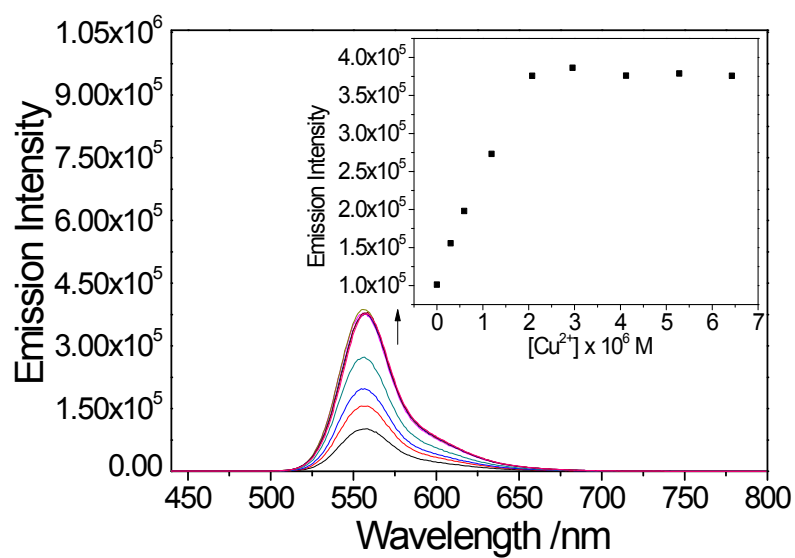


**Figure S21** Corrected emission spectra of **4** (11.8 μM) in acetonitrile at 298 K upon addition of various concentrations of Cu<sup>2+</sup>. Inset shows the plots of the emission intensity at 560 nm as a function of the concentration of Cu<sup>2+</sup>.

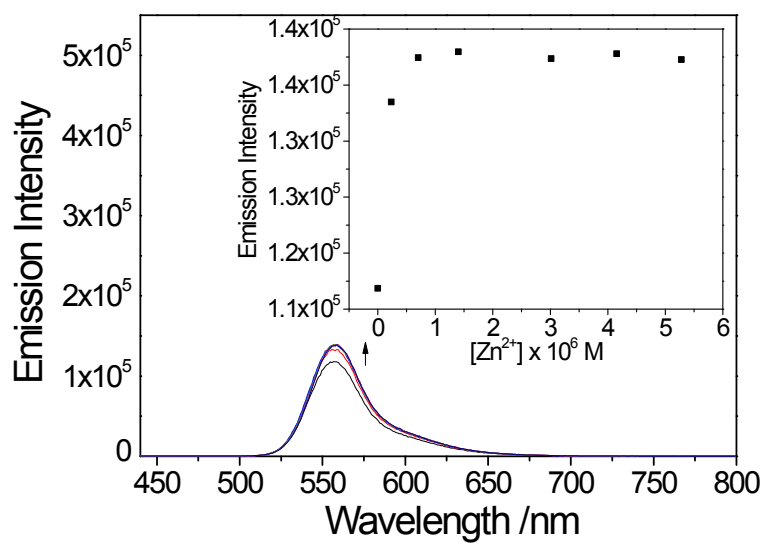


**Figure S22** Corrected emission spectra of **4** (11.8 μM) in acetonitrile at 298 K upon addition of various concentrations of Zn<sup>2+</sup>. Inset shows the plots of the emission intensity at 560 nm as a function of the concentration of Zn<sup>2+</sup>.



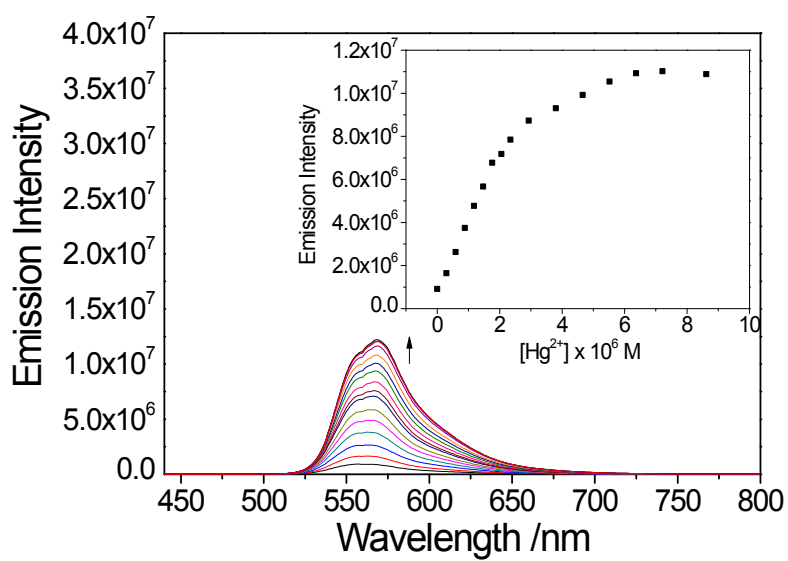


**Figure S23** Corrected emission spectra of **7** (11.7  $\mu\text{M}$ ) in acetonitrile at 298 K upon addition of various concentrations of  $\text{Hg}^{2+}$ . Inset shows the plots of the emission intensity at 560 nm as a function of the concentration of  $\text{Hg}^{2+}$ .

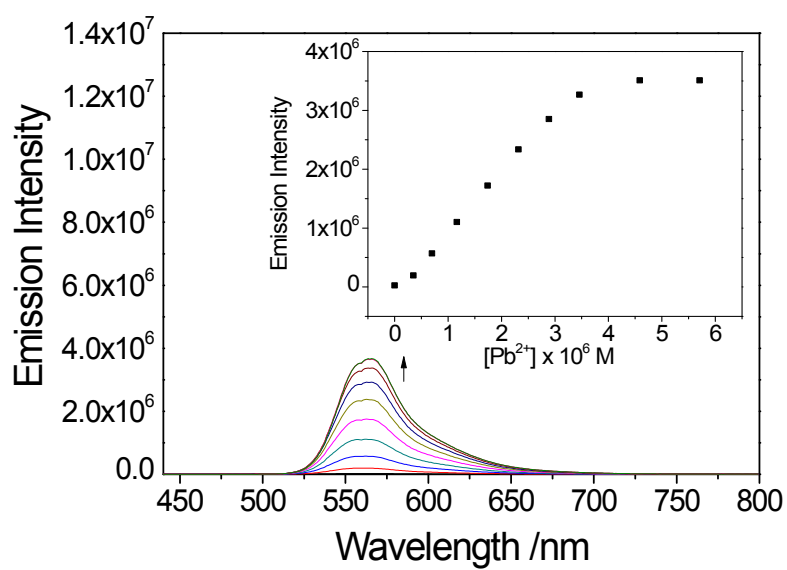


**Figure S24** Corrected emission spectra of **7** (11.7  $\mu\text{M}$ ) in acetonitrile at 298 K upon addition of various concentrations of  $\text{Pb}^{2+}$ . Inset shows the plots of the emission intensity at 560 nm as a function of the concentration of  $\text{Pb}^{2+}$ .

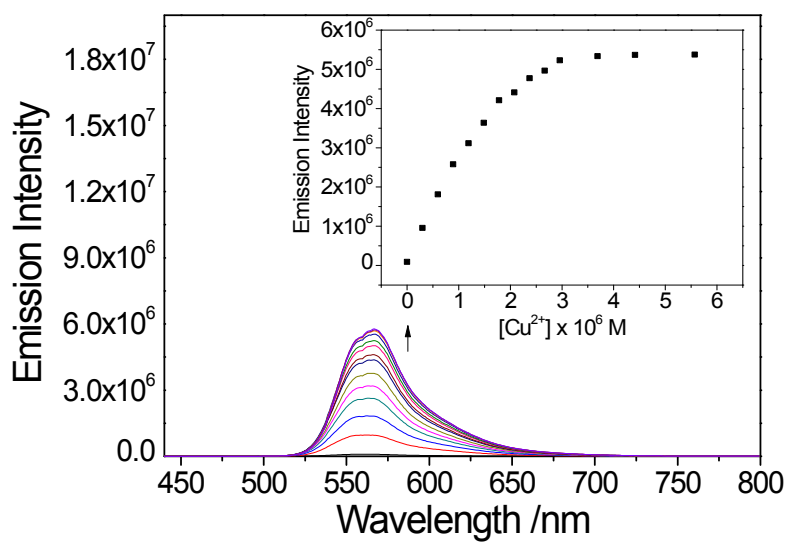


**Figure S25** Corrected emission spectra of **7** (11.7  $\mu\text{M}$ ) in acetonitrile at 298 K upon addition of various concentrations of  $\text{Cu}^{2+}$ . Inset shows the plots of the emission intensity at 560 nm as a function of the concentration of  $\text{Cu}^{2+}$ .